

# Characterization of Cellulose Acetate Membrane at Different Thicknesses on Sucrose Concentration by Forward Osmosis

*Aida I. Mohamad Idris*<sup>1</sup>

*Siti M. Mustapa Kamal*<sup>1,2</sup>

*Alifdalino Sulaiman*<sup>2</sup>

*Rozita Omar*<sup>3</sup>

*Munira Mohammad*<sup>1</sup>

<sup>1</sup>Centre for Water Research, Faculty of Engineering, Built Environment & Information Technology, SEGi University, 47810 Kota Damansara, Malaysia

<sup>2</sup>Department of Process and Food Engineering, Universiti Putra Malaysia, Serdang, Selangor 43400, Malaysia

<sup>3</sup>Department of Chemical and Environmental Engineering, Universiti Putra Malaysia, Serdang, Selangor 43400, Malaysia

\*e-mail: smazlina@upm.edu.my

*Submitted* 28 August 2022

*Revised* 6 December 2022

*Accepted* 13 December 2022

**Abstract.** Forward osmosis (FO) requires a specific membrane structure for applications like juice concentration. The phase inversion method was used to make cellulose acetate (CA) FO membranes. The solvents used were acetone and 1,4-dioxane. Additives included polyvinylpyrrolidone (PVP), methanol, and maleic acid were used in the preparation of CA membrane, which make it easier to improve a FO membrane's permeability. The performance of fabricated FO membrane and their morphology were evaluated with different casting thicknesses of 150, 200, and 250  $\mu\text{m}$ . Experiment works begins with an hour of membrane flux testing, deionized water was used as feed solution and 1 M NaCl as draw solution. The membrane was then used to concentrate 0.5 M sucrose with NaCl for 240 minutes (2 M). Contact angle, porosity, and scanning electron microscopy (SEM) were used to characterize membrane properties and morphology. High water flux (2.25  $\text{L}/\text{m}^2\text{hr}$ ) and high porosity (75.86%) were found at 200  $\mu\text{m}$  casting thickness. Water permeability of sucrose concentration at 200  $\mu\text{m}$  casting thickness had the highest flux (2.39  $\text{L}/\text{m}^2\text{hr}$ ). The results also show that flux values vary with membrane thickness. All membranes were hydrophilic with contact angles below  $90^\circ$ . A 200  $\mu\text{m}$  casting thickness produces a membrane with smooth and evenly distributed pores, according to morphology analysis. Structural parameter ( $S$ ) values had a proportional relationship with the FO membrane thickness, which thinner membrane potentially reduces the internal concentration polarization (ICP).

**Keywords:** Cellulose Acetate, Contact Angle, Forward Osmosis Membrane, Membrane Porosity, Membrane Thickness

## INTRODUCTION

A membrane technology called forward osmosis (FO) is activated by osmotic

pressures between 0 and 5 bar, which is lower than reverse osmosis (5-70 bar) and nanofiltration (5-40 bar) (Xu et al., 2017). Recently, researchers are attracted to the

advantage of the FO technology, where no externally applied hydraulic pressure is needed as the driving force of FO is the concentration difference between the feed and the draw solution (Yadav et al., 2020). In which the feed solution (FS) contains lower osmotic pressure, and the draw solution (DS) contains high osmotic pressure, separated by a semipermeable membrane (Chun et al., 2017). Common draw solutes used for the FO process are sodium chloride (NaCl) (Kim et al., 2019) and organic sugar (Babu et al., 2006). The draw solution selection depends on the osmotic pressure, required to have good chemical stability, compatibility with FO membrane, non-volatile and nontoxicity.

One of the important criteria for the FO process is the selection of a membrane (Rastogi, 2020). High mechanical strength, high water permeability, and high solute rejection are the best features of FO membrane. The common membrane material used for the FO process is cellulose acetate (Garcia-Castello et al., 2009, Shang and Baoli, 2018; Vaulina et al., 2018; Wenten et al., 2021). It has good mechanical strength, relatively high hydrophilicity, and low fouling affinity (Ahmed et al., 2021). Developing/fabricating an appropriate membrane structure for a specific application can improve the FO membrane's performance. The preparation of the FO membrane is through solution casting. In the casting process, a predetermined amount of polymer is blended with additives via the phase inversion method (using solvents). The additives in the casting solution are essential for FO membrane preparation because they can help in improving membrane performance. Studies by Malek et al. (2012) have shown that the hydrophilicity and permeability of FO membrane can be enhanced using polyvinylpyrrolidone (PVP) as

the additives. While Shang and Baoli (2018) have employed PVP, maleic acid, and methanol as additives to prepare FO membrane for concentrating the anthocyanin solution. Their results showed an improvement with a rejection rate of 98.61%. Another study by Chen et al. (2017) also used mixed additives for the FO membrane, resulting in improved membrane structure and properties. For polymer membranes, PVP allows morphological control in terms of thermodynamics and kinetics. It causes the structure of the polymer to be irregular and susceptible to phase separation in thermodynamics. By adding PVP, the phase differentiation/discretization of a high-viscosity polymer solution will produce a retarded and decelerated demixing process (Zhang et al., 2011). PVP also improves membrane selectivity by lowering the relative transport rate and reducing failures at the membrane surface (Rao et al., 2008).

Limitation of FO methods includes identifying suitable draw solution, issues with reverse solute flux and internal concentration polarization (ICP), this takes place in the membrane's porous support layer. ICP is generally affected by the support layer structure and thick dense membrane (Chia et al., 2020). ICP cannot be measured directly but the degree of ICP can be examined through the membrane structural parameter ( $S$ ).  $S$  relies on the membranes thickness, porosity and tortuosity. Chun et al. (2017) stated that FO membranes with thinner, more porous and less tortuous support layers resulted in a low value of  $S$  and higher water fluxes. The higher value of  $S$  indicates a more severe ICP problem (Niu et al., 2018). Reducing the membrane thickness could help in reducing ICP. Thus, an optimum balance is required to have high fluxes with the appropriate membrane structure, such as the

---

membrane thickness and porosity. Usually, membranes with thin thickness have less resistance to mass flow (Al-Obaidani et al., 2008). Good polymer dissolution in a solvent lead to effective interactions among the polymer and the solvent molecules (Mulder, 1996), which slow down solvent outflow during phase separation. As a result, nonsolvent inflow is allowed to diffuse more rapidly into the polymer matrix, resulting in a porous membrane and higher water flux.

FO membrane process has been utilized for concentrating fruit juice. Fruit juice concentration is one of the unit operations in food processing, which is performed to remove water to increase the shelf life that preserves the juice in long-term storage, reducing storage and transportation cost. Furthermore, FO can concentrate fruit juice without the need for high temperature or high pressure (Chanukya and Rastogi, 2017). FO membrane process is a non-thermal process alternative to the thermal-based or evaporation process commonly used for dehydrating or dewatering fruit juice or liquid foods. Thus, this process helps to reduce the thermal damage on the fruit juice that occurs during the evaporation process, promoting the high quality of juices by having retention of nutritional (such as antioxidants, polyphenols and vitamin), aroma, and flavor compounds (Rastogi, 2018).

One of the primary components available in fruit juice is sucrose (sugar). Concentrating sucrose are widely used in food engineering processes (Garcia-Castello et al., 2009). Hence, this study utilizes the FO membrane to concentrate sucrose to represent the fruit juice concentrating process. This work focused on fabricating the cellulose acetate (CA) forward osmosis membranes with the inclusion of PVP as the additives and casting at different thicknesses. The performances

and morphology of the fabricated FO membrane at different casting thicknesses were evaluated. The impact of thickness on the FO membrane properties in regard to water flux, morphology, porosity, contact angle and the structural parameter was studied. The membrane casting thickness is evaluated in order to obtain the limitation of the membrane permeability and resistance to the sucrose solution.

## MATERIALS AND METHODS

### Chemicals

Cellulose acetate (CA) (39.8 wt% acetyl, MW 30,000 g/mol) was obtained from Sigma Aldrich. 1,4-dioxane, maleic acid, methanol, polyvinylpyrrolidone (PVP-K30), and acetone were analytical grade obtained from a local supplier. All these chemicals were used without further purification. Deionised (DI) water was used in the coagulation process.

### Preparation of CA-FO Membrane Dope

Phase inversion approach was used to prepare the CA-FO membrane, which was done in accordance with Shang and Baoli's method (2018). The casting solution contains 13% CA, 3% PVP, 2% maleic acid, 45% 1,4-dioxane, 31% acetone, and 6% methanol. The fabrication of CA-FO membrane is shown in Figure 1. For 24 hours, the fully dissolved dope solution was maintained at room temperature to remove air bubbles and stop the development of defects. This solution was cast on a glass plate surface and a proper thickness was adjusted at 150, 200, 250  $\mu\text{m}$  by using a casting knife (Zechner-Swiss) at a constant speed. The membrane was partially evaporated for 60 seconds under atmospheric conditions and then immersed in a coagulation water. To remove any remaining organic solvents from the

coagulated membranes, they were submerged in tap water overnight.

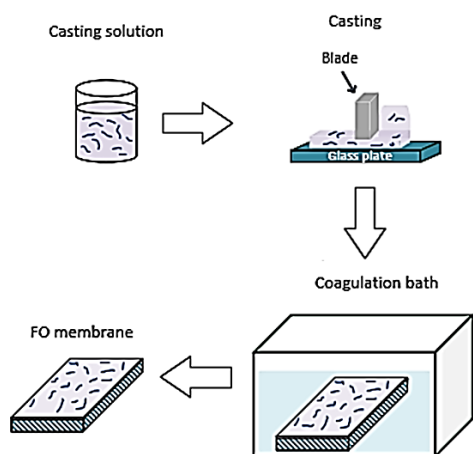


**Fig. 1:** Fabrication of CA-FO membrane

### Membrane Performance

The FO system consist of peristaltic pump, electronic balance, magnetic stirrer and EC meter as shown in Figure 2. Counter current cross-flow was used, and both feed solution (FS) and draw solution (DS) flowed in a closed loop. In this study, AL-FS mode is applied where the membrane is placed with its active layer facing the concentrated feed solution and the support layer facing the permeate side. The effective area of membranes was 28 cm<sup>2</sup>, and the FS flowed on the active layer of the membrane. Prior to conducting permeation testing, the membrane was compacted with deionized water for an hour at constant operating pressure to ensure the stability of the FO membrane and to produce a consistent flow. The water flux test was carried out in 60 minutes using DI water as FS and 1 M NaCl as DS flowed at a constant flowrate of 1.4 L/min. The FO process continued with the evaluation of sucrose using different concentrations of DS (2 M NaCl) and FS (0.5 M sucrose solution). This procedure was extended for up to 240 min.

The electrolytic conductivity (EC) values

of feed solution were measured by an EC meter (Hanna) throughout the experiment. The pure water flux ( $J_w$ ) was calculated by the permeate volume per unit time and effective area as in Eq. (1).

$$J_w = \frac{\Delta V_{draw}}{A_m \times t} \quad (1)$$

where  $\Delta V_{draw}$  is the volume change,  $A_m$  is the effective membrane surface area and  $t$  is time. Each run is duplicated.

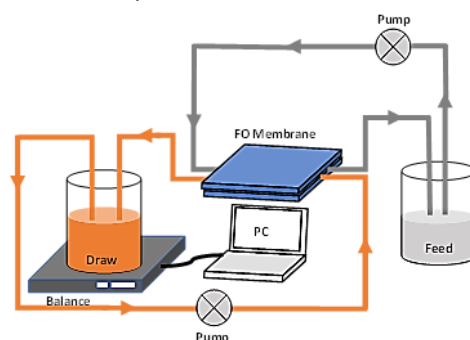


**Fig. 2:** Schematic diagram of the forward osmosis system

### Morphological Analysis using Scanning Electron Microscopy (SEM)

The surface topography of the fabricated membrane was analysed using SEM (JEOL Ltd, Singapore). Sample mounted on a specimen stage using a conductive adhesive and coated with electrically conducting material (gold), 20Ma. Scans were obtained with an electron accelerating voltage of 10 kV.

### Porosity

The average porosity of the membranes was measured using gravimetric method according to (Chan et al., 2018). Pore volume was divided by total volume as in Eq. (2).

$$\varepsilon = \frac{(w_0 - w_1)/\rho_{water}}{(w_0 - w_1)/\rho_{water} + w_1/\rho_p} \times 100\% \quad (2)$$

where  $\varepsilon$  is the membrane porosity.  $w_0$  and  $w_1$  are the weights of wet and dried membranes (g), respectively.  $\rho_p$  and  $\rho_{water}$  are the densities

of CA ( $1.3 \text{ g/cm}^3$ ) and water ( $1.0 \text{ g/cm}^3$ ) at  $25^\circ\text{C}$ , respectively. The result was the average value of at least five parallel measurements.

### Contact Angle

Water contact angle measurements determined the membranes hydrophilicity at room temperature. A membrane sample of  $1 \times 5 \text{ cm}^2$  was mounted to a glass slide, and then  $2.0 \mu\text{L}$  of distilled water was poured onto the membrane's air-side surface (Figure 3). Speed optimum video measurement technology recorded the water contact angle decaying with drop age. At least five measurements were averaged to get a reliable value.

### Structural Parameter (S)

Structural parameter can be used to describe the severity of the ICP and have been expressed in Eq.(3).

$$S = \frac{D\tau}{\varepsilon} \quad (3)$$

where,  $D$  is the thickness,  $\tau$  is the tortuosity and  $\varepsilon$  is the porosity.

### Statistical Analysis

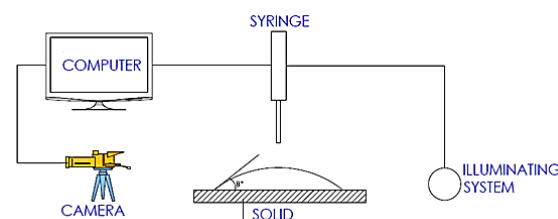
All statistical analysis was carried out with Microsoft excel. Correlations were considered statistically significant at a confidence interval  $P < 0.05$ .

## RESULTS AND DISCUSSION

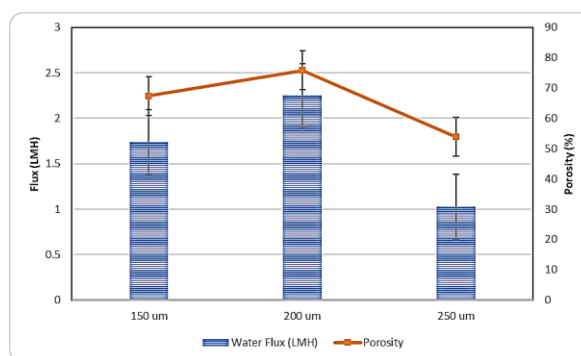
### Membrane Performance: Fluxes

Figure 4 shows the water flux of FO membranes prepared at different casting thicknesses of 150, 200, and 250  $\mu\text{m}$ . The porosity increased from 53.91% to 75.86%, with a membrane casting thickness of 250  $\mu\text{m}$   $<$  150  $\mu\text{m}$   $<$  200  $\mu\text{m}$ . Low membrane thickness has less resistance to mass transport (Al-Obaidani et al, 2008; Chan et al,

2018), but the combination of membrane thickness and porosity is also crucial to permeate flux. Thus, it can be observed that the highest water flux ( $2.25 \text{ L/m}^2 \text{ hr}$  (LMH)) was found at a membrane casting thickness of 200  $\mu\text{m}$  with high porosity (75.86%). Due to a chemical potential difference, as a casting film is submerged in the coagulation bath, diffusions of solvent (outflow) and nonsolvent (inflow) in the polymer matrix occur. Strong contacts between a polymer and the solvent molecules result from an effective dissolution of the polymer, which slows the solvent's outflow during phase separation. Therefore, the inflow of nonsolvent is allowed to diffuse into the polymer matrix more rapidly, producing more porous membranes and higher water flux.



**Fig. 3:** Schematic diagram of contact angle measurement



**Fig. 4:** Membrane water flux at different thickness and porosity

Decrease casting thickness facilitated water flux because thinner membranes showed less resistance against water and salt

transport (Nguyen et al., 2013). Although the membrane casting thickness of 150  $\mu\text{m}$  was thin, the porosity was slightly lower (67.45%) than 200  $\mu\text{m}$ . High porosity means a more porous membrane surface, which has a higher effective molecular diffusion (Al-Obaidani et al., 2008) and induces more water flux (Nguyen, 2013). In contrast, a membrane casting thickness of 250  $\mu\text{m}$  has the lowest value of water flux (1.03 LMH) with 53.41% porosity. During casting for membrane thickness of 250  $\mu\text{m}$ , agglomeration could occur; therefore, pore formation might be distorted and affecting porosity. This allows a dense polymer layer to close the void, eventually reducing the porosity. Surface images of the membrane observed from SEM (Figure 6 a-c) confirm that the membrane casting thickness of 250  $\mu\text{m}$  has less and a small pore than the image of the pore of 150 and 200  $\mu\text{m}$  membrane casting thickness.

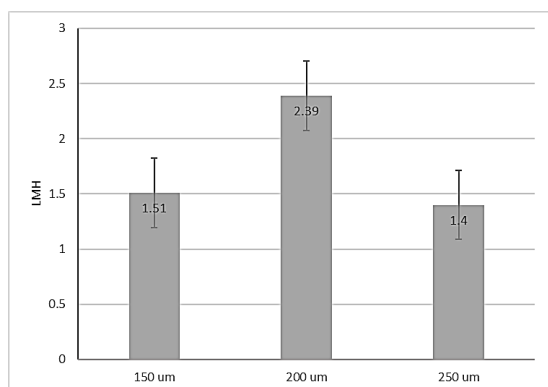


**Fig. 5:** Sucrose concentration evaluation at different membrane thickness

After one hour of water flux test using 1 M NaCl as DS and DI as the FS, the FO process was continued using different concentrations of DS (2 M NaCl) and FS (0.5 M sucrose solution). This is to observe the concentration of the sucrose solution, which the permeation test was prolonged up to 240 min. As a result, permeate flux from sucrose solution (Figure 5) was observed to rise from 1.51 LMH

(thickness 150  $\mu\text{m}$ ) to 2.39 LMH (thickness 200  $\mu\text{m}$ ), which was slightly higher than permeate flux of water (2.25 LMH). In contrast, at 250  $\mu\text{m}$  the permeate flux from sucrose solution decreased to 1.4 LMH, with the water flux reduced to 1.03 LMH. These results are associated with the low porous membrane surface at thickness of 250  $\mu\text{m}$  (53.41% porosity). Results demonstrated that 200  $\mu\text{m}$  is producing the highest flux. This is due to the porous structure developed at this thickness which is suitable for the separation of phases between sucrose and NaCl. Water flux is greatly influenced by the support layer (ICP phenomenon). The FO operating state cannot be tuned to control external concentration polarisation (ECP) and internal concentration polarisation (ICP). In order to improve the structural parameters (thickness, porosity, and tortuosity), membranes with low ICP must be constructed using the support layer's structure and hydrophilicity. By constructing a very thin support layer, ICP can be reduced, but weak mechanical strength is a problem. Thickness of the membrane is also directly influenced by the solute's diffusion coefficient,  $K$ , which comes from the bulk ( $D$ ). A thinner and looser support layer is likewise associated with a lower  $K$  value. Thinner membrane improved ICP during phase separation. Reducing the overall osmotic pressure differential between FS and DS in order to lessen water flux, which is the main concern with ICP. Therefore, 200  $\mu\text{m}$  membrane thickness was suggested for CA-FO membrane for concentrating sucrose.

### Membrane Surface Morphology

The top surface layer of membranes of all thickness is shown in Figure 6. A clear void fraction can be observed on the membrane surface in Figures 6(a) (150  $\mu\text{m}$ ) and (b) (200  $\mu\text{m}$ ), indicating a more porous structure.

However, smooth and well-distributed pores are observed for the membrane surface at a thickness of 200  $\mu\text{m}$ . In Figure 6(c), for membrane thickness of 250  $\mu\text{m}$  less void fraction was sighted, implying a less porous structure. The pore distribution (Figure 6(c)) was not well distributed and smooth, with some pore distances being quite far. The type of polymer used, as well as the compatibility of solvent and pore performing agent, are all important factors in pore formation. The phase inversion procedure converts the dope polymer from a liquid to a solid. Controlling the pore diameter of the membrane is crucial for preserving selectivity during membrane fabrication. As a result, it is critical to formulating the membrane with the right amount of pore performing agent.

Fouling on the membrane surface is the main issue the FO process. Reduced membrane permeability, which results in process inefficiency, can be linked to build up of foulants on the membrane surface and/or inside the pores (Lee et al., 2020). Thus, the fouling on the CA-FO membrane surface's active layer that faces the flow of sucrose solution (FS) was analysed (Figure 6 d – f). The scales for Figure 6 (a-c) are 10  $\mu\text{m}$ , whereas for Figure 6 (d-f) are 50  $\mu\text{m}$ . As water diffuses into the membrane and flows towards the DS, the changes in concentration causing internal concentration of polarisation occur in the porous support layer, therefore reducing water flux, eventually becoming the potential foulant. Hence, positioned with the active layer facing FS, fouling occurs with the foulant (sucrose molecules) deposited on the membrane surface, blocking the pore. Then, the fouling layer was developed over time, covering the pore. It was observed from the image (d-f) the membrane pore is not visible. The foulant may have caused a layer on the membrane surface.

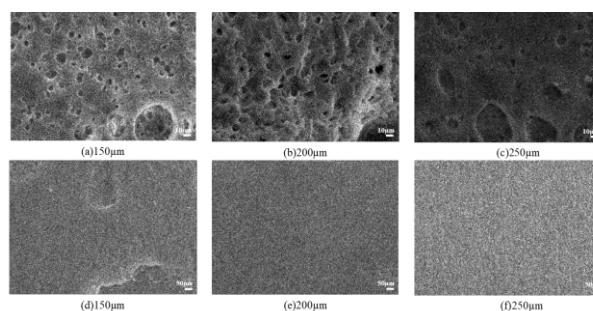


**Fig. 6:** SEM images of a new fabricated CA-FO membrane (first row) (magnification 5000); (a) 150  $\mu\text{m}$ , (b) 200  $\mu\text{m}$ , (c) 250  $\mu\text{m}$ , and images of CA-FO membrane after the FO process (second row) (magnification 1000); (d) 150  $\mu\text{m}$  (e) 200  $\mu\text{m}$  (f) 250  $\mu\text{m}$ .

### Water Contact Angle and Structural Parameter

Using a contact angle measurement device, the produced membranes' surface hydrophilicity was determined. The increase in membrane hydrophilicity was correlated with a reduction in the water contact angle. The water contact angle of FO membranes was in the range of 60 to 61°, which shows good hydrophilic properties. Table 1 shows the results of the contact angle of each three different membrane thicknesses. The contact angle of the membranes was 61° (150  $\mu\text{m}$ ), 61° (200  $\mu\text{m}$ ), and 60° (250  $\mu\text{m}$ ). All three membranes were considered hydrophilic surfaces with the order of 200, 150, and 250  $\mu\text{m}$  according to the porosity data (Figure 2). Etemadi et. al (2019) also fabricated CA membrane with a hydrophilic surface. The formulation of their CA membrane was using a slightly high amount of CA polymer (17.5%) obtained a contact angle of 65.4° with respective 76.7 % porosity for a membrane casting thickness of 200  $\mu\text{m}$ .

In this study, membrane thickness of 200 and 150  $\mu\text{m}$  that have high porosity values (75.86% and 67.45%) are interrelated with a slightly higher degree of contact angle (61°)

as compared to contact angle for membrane thickness 250  $\mu\text{m}$  ( $60^\circ$ ). It was observed that a membrane with a high contact angle ( $61^\circ$ ) has high water and sucrose flux (Figures 2 and 3). This situation might occur because the membrane has high porosity, although it has high contact angle or hydrophilic membrane surface. In contrast with the statement by Kumar and Ismail (2015) which states that a lower contact angle has a high affinity toward the water. This study indicates that the flux performance relies not only on the hydrophilic surface but on other properties such as porosity.

**Table 1.** Contact angle, structural parameters ( $S$ ) and porosity for CA membrane

Membrane casting thickness ( $\mu\text{m}$ )	Contact angle ( $^\circ$ )	Structural parameters ( $\mu\text{m}$ )	Porosity (%)
150	61	258	67.45
200	61	296	75.86
250	60	577	53.41
CA	65.4	-	76.7

(Etemadi et al., 2019)

The  $S$  values for this study were calculated and shown in Table 1. The results shown that the thin membranes (150 and 200  $\mu\text{m}$ ) indicates lower  $S$  values (258 and 298  $\mu\text{m}$ , respectively) with higher water fluxes (results in Figure 4) as compared to 250  $\mu\text{m}$  membrane. Niu et. al. (2018) state that higher  $S$  values mean serious ICP problem. Reducing the FO membrane thickness could help in lowering ICP issue. Therefore, from this study, it is possible that fabricated FO membranes at casting thickness of 200  $\mu\text{m}$  or below could have less ICP problem.

## CONCLUSIONS

In this study, the phase inversion was used to fabricate the CA-FO membrane at different thicknesses. It was evident that membrane thickness is a critical parameter influencing flux performance. The findings have demonstrated that thinner membranes (150 and 200  $\mu\text{m}$ ) have higher water permeability and lower  $S$  values. The highest water and sucrose fluxes were confirmed at the thickness of 200  $\mu\text{m}$  with the highest porosity. All the fabricated membranes were classified as hydrophilic due to the contact values below  $90^\circ$ . It has been shown that an appropriate combination of the hydrophilic membrane surface with porosity properties is essential to influence the flux performance. Thus, a proper membrane fabrication technique such as changing the membrane surface properties (membrane thickness and porosity) could enhance the performance of the FO process and possible to reduce the ICP.

## ACKNOWLEDGEMENT

The authors acknowledge the Universiti Putra Malaysia (Vot: 9300454) and Segi University Sdn. Bhd. (SEGiIRF/2019-7/FoEBE-27/90) for the study and financial support through a matching grant.

## REFERENCES

- Ahmed, D. F., Isawi, H., Badway, N. A., Elbayaa, A. A., & Shawky, H., 2021. "Graphene oxide incorporated cellulose triacetate/cellulose acetate nanocomposite membranes for forward osmosis desalination." *Arabian J. of Chem.*, 14(3), 102995. doi:10.1016/j.arabjc.2021.102995

- Al Obaidani, S., Curcio, E., Macedonio, F., Diprofito, G., Al Hinai, H., and Drioli, E., 2008. "Potential of membrane distillation in seawater desalination: Thermal efficiency, sensitivity study and cost estimation." *J. of Membr. Sci.*, 323(1), 85–98. doi:10.1016/j.memsci.2008.06.006
- Babu, B. R, Rastogi N.K., and Raghavarao, K.S.M.S., 2006. "Effect of process parameters on transmembrane flux during direct osmosis." *J. of Membr. Sci.*, 280(1-2),185-194. Doi:10.1016/j.memsci.2006.01.018
- Chan, M. K., Ong, C. S., and Kumaran, P., 2018. "Development and characterization of glycerol coating on the PAN/PVDF composite membranes." *IOP Conference Series: Materials Science and Engineering*, 458, 012006. doi:10.1088/1757-899x/458/1/012006
- Chanukya, B. S., and Rastogi, N. K., 2017. "Ultrasound assisted forward osmosis concentration of fruit juice and natural colorant." *Ultrason. Sonochem.*, 34, 426–435. Doi:10.1016/j.ultsonch.2016.06.020
- Chen, X., Xu, J., Lu, J., Shan, B., and Gao, C., 2017. "Enhanced performance of cellulose triacetate membranes using binary mixed additives for forward osmosis desalination." *Desalination*, 405, 68–75. doi:10.1016/j.desal.2016.12.003
- Chia, W. Y., Khoo, K. S., Chia, S. R., Chew, K. W., Yew, G. Y., Ho, Y.-C., Show, P.L., and Chen, W.-H., 2020. "Factors affecting the performance of membrane osmotic processes for bioenergy development." *Energies*, 13(2), 481. doi:10.3390/en13020481
- Chun, Y., Mulcahy, D., Zou, L., and Kim, I., 2017. "A short review of membrane fouling in forward osmosis processes." *Membr.*, 7(2),30. doi:10.3390/membranes7020030
- Etemadi, H., Yegani, R., and Seyfollahi, M., 2017. "The effect of amino functionalized and polyethylene glycol grafted nanodiamond on anti-biofouling properties of cellulose acetate membrane in membrane bioreactor systems. *Sep. and Purif. Technol.*,177,350–362. doi:10.1016/j.seppur.2017.01.013
- Garcia-Castello, E. M., McCutcheon, J. R., and Elimelech, M., 2009. "Performance evaluation of sucrose concentration using forward osmosis." *J. of Membr. Sci.*, 338(1-2), 61–66. doi:10.1016/j.memsci.2009.04.011
- Kumar, R., and Ismail, A. F., 2015. "Fouling control on microfiltration/ultrafiltration membranes: Effects of morphology, hydrophilicity, and charge." *J. of Appl. Polym. Sci.*, 132(21), n/a–n/a. doi:10.1002/app.42042
- Kim, D.I, Gwak, G., Zhan, M., and Hong, S., 2019. "Sustainable dewatering of grapefruit juice through forward osmosis: Improving membrane performance, fouling control, and product quality." *J. of Membr. Sci.*,578, 53-60. doi:10.1016/j.memsci.2019.02031
- Lee, W. J., Ng, Z. C., Hubadillah, S. K., Goh, P. S., Lau, W. J., Othman, M. H. D., Ismail, A.F., and Hilal, N., 2020. "Fouling mitigation in forward osmosis and membrane distillation for desalination." *Desalination*, 480, 114338. doi:10.1016/j.desal.2020.114338
- Mulder, M., 1996. *Basic Principles of Membrane Technology*. Springer.

- doi:10.1007/978-94-009-1766-8
- Malek, S. A. A, Abu Seman, M. N., Johnson, D., and Hilal, N., 2012. "Formation and characterization of polyethersulfone membranes using different concentrations of polyvinyl pyrrolidone." *Desalination*, 288, 31–39. doi:10.1016/j.desal.2011.12.006
- Nguyen, T. P. N., Yun, E.-T., Kim, I.-C., and Kwon, Y.-N., 2013. "Preparation of cellulose triacetate/cellulose acetate (CTA/CA)-based membranes for forward osmosis." *J. of Membr. Sci.*, 433, 49–59. doi:10.1016/j.memsci.2013.01.027
- Niu, F., Huang, M., Cai, T., and Meng, L., 2018. "Effect of membrane thickness on properties of FO membranes with nanofibrous substrate." *IOP Conf. Series: Earth and Environmental Science*, 170(5), (052005). doi: 10.1088/1755-1315/170/5/052005
- Rao, P. S., Wey, M.-Y., Tseng, H.-H., Kumar, I. A., and Weng, T.-H., 2008. "A comparison of carbon/nanotube molecular sieve membranes with polymer blend carbon molecular sieve membranes for the gas permeation application." *Microporous and Mesoporous Mater.*, 113(1-3), 499–510. doi:10.1016/j.micromeso.2007.12.008
- Rastogi, N. K., 2018. "Reverse osmosis and forward osmosis for the concentration of fruit juices." *Fruit Juices*, 241–259. doi:10.1016/b978-0-12-802230-6.00013-8
- Rastogi, N. K., 2020. "Applications of forward osmosis process in food processing and future implications." *Current Trends and Future Developments on (Bio-) Membr.*, 113–138. doi:10.1016/b978-0-12-816777-9.00005-8
- Shang, M., and Shi, B., 2018. "Study on preparation and performances of cellulose acetate forward osmosis membrane." *Chem. Pap.*, 72(12), 3159–3167. doi:10.1007/s11696-018-0554-z
- Vaulina, E., Widyaningsih, S., Kartika, D., and Romdoni, M. P., 2018. "The effect of cellulose acetate concentration from coconut nira on ultrafiltration membrane characters." *IOP Conference Series: Materials Science and Engineering*, 349, 012020. doi:10.1088/1757-899x/349/1/012020
- Wenten, I. G., Khoiruddin, K., Reynard, R., Lugito, G., and Julian, H., 2021. "Advancement of forward osmosis (FO) membrane for fruit juice concentration." *J. of Food Eng.*, 290, 110216. doi:10.1016/j.jfoodeng.2020.110216
- Xu, W., Chen, Q., and Ge, Q., 2017. "Recent advances in forward osmosis (FO) membrane: Chemical modifications on membranes for FO processes." *Desalination*, 419, 101–116. doi:10.1016/j.desal.2017.06.007
- Yadav, S., Ibrar, I., Bakly, S., Khanafer, D., Altaee ,A., Padmanaban, V.C., Samal, A.K, and Hawari, A.H., 2020. "Organic fouling in forward osmosis: A comprehensive review," *Water* 12(5), 1505. doi:10.3390/w12051505
- Zhang, P., Wang, Y., Xu, Z., and Yang, H., 2011. "Preparation of poly (vinyl butyral) hollow fiber ultrafiltration membrane via wet-spinning method using PVP as additive." *Desalination*, 278(1-3), 186–193. doi:10.1016/j.desal.2011.05.026
-